

## CHAPTER 1

# Introduction

### 1.1 THE LIQUID STATE

The liquid state of matter is intuitively perceived as being intermediate in nature between a gas and a solid. Thus a natural starting point for discussion of the properties of any given substance is the relationship between pressure  $P$ , number density  $\rho$  and temperature  $T$  in the different phases, summarised in the equation of state  $f(P, \rho, T) = 0$ . The phase diagram in the  $\rho$ – $T$  plane typical of a simple, one-component system is sketched in Figure 1.1. The region of existence of the liquid phase is bounded above by the critical point (subscript c) and below by the triple point (subscript t). Above the critical point there is only a single fluid phase, so a continuous path exists from liquid to fluid to vapour; this is not true of the transition from liquid to solid, because the solid–fluid coexistence line, or melting curve, does not terminate at a critical point. In many respects the properties of the dense, supercritical fluid are not very different from those of the liquid, and much of the theory we develop in later chapters applies equally well to the two cases.

We shall be concerned in this book almost exclusively with classical liquids. For atomic systems a simple test of the classical hypothesis is provided by the value of the de Broglie thermal wavelength  $\Lambda$ , defined as

$$\Lambda = \left( \frac{2\pi\beta\hbar^2}{m} \right)^{1/2} \quad (1.1.1)$$

where  $m$  is the mass of an atom and  $\beta = 1/k_B T$ . To justify a classical treatment of static properties it is necessary that  $\Lambda$  be much less than  $a$ , where  $a \approx \rho^{-1/3}$  is the mean nearest-neighbour separation. In the case of molecules we require, in addition, that  $\Theta_{\text{rot}} \ll T$ , where  $\Theta_{\text{rot}} = \hbar^2/2Ik_B$  is a characteristic rotational temperature ( $I$  is the molecular moment of inertia). Some typical results are shown in Table 1.1, from which we see that quantum effects should be small for all the systems listed, with the exceptions of hydrogen and neon.

Use of the classical approximation leads to an important simplification, namely that the contributions to thermodynamic properties which arise from thermal motion can be separated from those due to interactions between particles. The separation of kinetic and potential terms suggests a simple means of characterising the liquid state. Let  $V_N$  be the total potential energy of a system, where  $N$  is the number of particles, and let  $K_N$  be the total

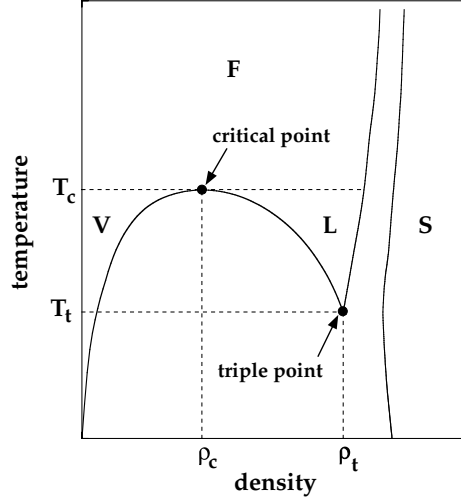


FIG. 1.1. Schematic phase diagram of a typical monatomic substance, showing the boundaries between solid (S), liquid (L) and vapour (V) or fluid (F) phases.

TABLE 1.1. *Test of the classical hypothesis*

Liquid	$T_t/\text{K}$	$\Lambda/\text{\AA}$	$\Lambda/a$	$\Theta_{\text{rot}}/T_t$
H <sub>2</sub>	14.1	3.3	0.97	6.1
Ne	24.5	0.78	0.26	
CH <sub>4</sub>	91	0.46	0.12	0.083
N <sub>2</sub>	63	0.42	0.11	
Li	454	0.31	0.11	0.094
Ar	84	0.30	0.083	
HCl	159	0.23	0.063	
Na	371	0.19	0.054	
Kr	116	0.18	0.046	0.001
CCl <sub>4</sub>	250	0.09	0.017	

$\Lambda$  is the de Broglie thermal wavelength at  $T = T_t$  and  $a = (V/N)^{1/3}$ .

kinetic energy. Then in the liquid state we find that  $K_N/|V_N| \approx 1$ , whereas  $K_N/|V_N| \gg 1$  corresponds to the dilute gas and  $K_N/|V_N| \ll 1$  to the low-temperature solid. Alternatively, if we characterise a given system by a length  $\sigma$  and an energy  $\varepsilon$ , corresponding roughly to the range and strength of the intermolecular forces, we find that in the liquid region of the phase diagram the reduced number density  $\rho^* = N\sigma^3/V$  and reduced temperature  $T^* = k_B T/\varepsilon$  are both of order unity. Liquids and dense fluids are also distinguished from dilute gases by the greater importance of collisional processes and short-range, positional correlations, and from solids by the lack of long-range order; their structure is in many

TABLE 1.2. *Selected properties of typical simple liquids*

Property	Ar	Na	N <sub>2</sub>
$T_t/K$	84	371	63
$T_b/K$ ( $P = 1$ atm)	87	1155	77
$T_c/K$	151	2600	126
$T_c/T_t$	1.8	7.0	2.0
$\rho_t/\text{nm}^{-3}$	21	24	19
$C_P/C_V$	2.2	1.1	1.6
$L_{\text{vap}}/\text{kJ mol}^{-1}$	6.5	99	5.6
$\chi_T/10^{-12} \text{ cm}^2 \text{ dyn}^{-1}$	200	19	180
$c/\text{m s}^{-1}$	863	2250	995
$\gamma/\text{dyn cm}^{-1}$	13	191	12
$D/10^{-5} \text{ cm}^2 \text{ s}^{-1}$	1.6	4.3	1.0
$\eta/\text{mg cm}^{-1} \text{ s}^{-1}$	2.8	7.0	3.8
$\lambda/\text{mW cm}^{-1} \text{ K}^{-1}$	1.3	8800	1.6
$(k_B T/2\pi D\eta)/\text{\AA}$	4.1	2.7	3.6

$\chi_T$  = isothermal compressibility,  $c$  = speed of sound,  $\gamma$  = surface tension,  $D$  = self-diffusion coefficient,  $\eta$  = shear viscosity and  $\lambda$  = thermal conductivity, all at  $T = T_t$ ;  $L_{\text{vap}}$  = heat of vaporisation at  $T = T_b$ .

cases dominated by the “excluded-volume” effect associated with the packing together of particles with hard cores.

Selected properties of a simple monatomic liquid (argon), a simple molecular liquid (nitrogen) and a simple liquid metal (sodium) are listed in Table 1.2. Not unexpectedly, the properties of the liquid metal are in certain respects very different from those of the other systems, notably in the values of the thermal conductivity, isothermal compressibility, surface tension, heat of vaporisation and the ratio of critical to triple-point temperatures; the source of these differences should become clear in Chapter 10. The quantity  $k_B T/2\pi D\eta$  in the table provides a Stokes-law estimate of the particle diameter.

## 1.2 INTERMOLECULAR FORCES AND MODEL POTENTIALS

The most important feature of the pair potential between atoms or molecules is the harsh repulsion that appears at short range and has its origin in the overlap of the outer electron shells. The effect of these strongly repulsive forces is to create the short-range order that is characteristic of the liquid state. The attractive forces, which act at long range, vary much more smoothly with the distance between particles and play only a minor role in determining the structure of the liquid. They provide, instead, an essentially uniform, attractive background and give rise to the cohesive energy that is required to stabilise the liquid. This separation of the effects of repulsive and attractive forces is a very old-established concept. It lies at the heart of the ideas of van der Waals, which in turn form the basis of the very successful perturbation theories of the liquid state that we discuss in Chapter 5.

The simplest model of a fluid is a system of hard spheres, for which the pair potential  $v(r)$  at a separation  $r$  is

$$\begin{aligned} v(r) &= \infty, & r < d, \\ &= 0, & r > d \end{aligned} \quad (1.2.1)$$

where  $d$  is the hard-sphere diameter. This simple potential is ideally suited to the study of phenomena in which the hard core of the potential is the dominant factor. Much of our understanding of the properties of the hard-sphere model come from computer simulations. Such calculations have revealed very clearly that the structure of a hard-sphere fluid does not differ in any significant way from that corresponding to more complicated interatomic potentials, at least under conditions close to crystallisation. The model also has some relevance to real, physical systems. For example, the osmotic equation of state of a suspension of micron-sized silica spheres in an organic solvent matches almost exactly that of a hard-sphere fluid.<sup>1</sup> However, although simulations show that the hard-sphere fluid undergoes a freezing transition at  $\rho^*$  ( $= \rho d^3$ )  $\approx 0.945$ , the absence of attractive forces means that there is only one fluid phase. A simple model that can describe a true liquid is obtained by supplementing the hard-sphere potential with a square-well attraction, as illustrated in Figure 1.2(a). This introduces two additional parameters:  $\varepsilon$ , the well depth, and  $(\gamma - 1)$ , the width of the well in units of  $d$ , where  $\gamma$  typically has a value of about 1.5. An alternative to the square-well potential with features that are of particular interest theoretically is the hard-core Yukawa potential, given by

$$\begin{aligned} v(r) &= \infty, & r^* < 1, \\ &= -\frac{\varepsilon}{r^*} \exp[-\lambda(r^* - 1)], & r^* > 1 \end{aligned} \quad (1.2.2)$$

where  $r^* = r/d$  and the parameter  $\lambda$  measures the inverse range of the attractive tail in the potential. The two examples plotted in Figure 1.2(b) are drawn for values of  $\lambda$  appropriate either to the interaction between rare-gas atoms ( $\lambda = 2$ ) or to the short-range, attractive forces<sup>2</sup> characteristic of certain colloidal systems ( $\lambda = 8$ ).

A more realistic potential for neutral atoms can be constructed by a detailed quantum-mechanical calculation. At large separations the dominant contribution to the potential comes from the multipolar dispersion interactions between the instantaneous electric moments on one atom, created by spontaneous fluctuations in the electronic charge distribution, and moments induced in the other. All terms in the multipole series represent attractive contributions to the potential. The leading term, varying as  $r^{-6}$ , describes the dipole-dipole interaction. Higher-order terms represent dipole-quadrupole ( $r^{-8}$ ), quadrupole-quadrupole ( $r^{-10}$ ) interactions, and so on, but these are generally small in comparison with the term in  $r^{-6}$ .

A rigorous calculation of the short-range interaction presents greater difficulty, but over relatively small ranges of  $r$  it can be adequately represented by an exponential function of the form  $\exp(-r/r_0)$ , where  $r_0$  is a range parameter. This approximation must be supplemented by requiring that  $v(r) \rightarrow \infty$  for  $r$  less than some arbitrarily chosen, small value. In practice, largely for reasons of mathematical convenience, it is more usual to represent the short-range repulsion by an inverse-power law, i.e.  $r^{-n}$ , with  $n$  lying generally in the

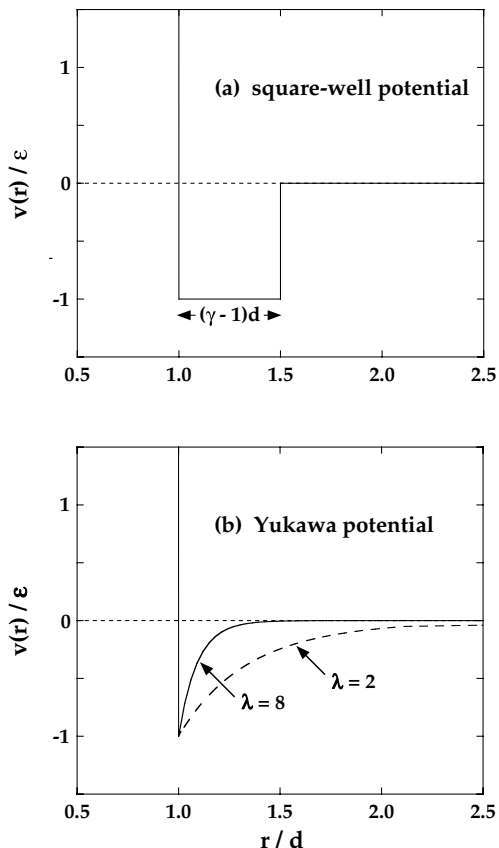


FIG. 1.2. Simple pair potentials for monatomic systems. See text for details.

range 9 to 15. The behaviour of  $v(r)$  in the limiting cases  $r \rightarrow \infty$  and  $r \rightarrow 0$  may therefore be incorporated in a simple potential function of the form

$$v(r) = 4\epsilon \left[ (\sigma/r)^{12} - (\sigma/r)^6 \right] \quad (1.2.3)$$

which is the famous 12-6 potential of Lennard-Jones. Equation (1.2.3) involves two parameters: the collision diameter  $\sigma$ , which is the separation of the particles where  $v(r) = 0$ ; and  $\epsilon$ , the depth of the potential well at the minimum in  $v(r)$ . The Lennard-Jones potential provides a fair description of the interaction between pairs of rare-gas atoms and also of quasi-spherical molecules such as methane. Computer simulations<sup>3</sup> have shown that the triple point of the Lennard-Jones fluid is at  $\rho^* \approx 0.85$ ,  $T^* \approx 0.68$ .

Experimental information on the pair interaction can be extracted from a study of any process that involves collisions between particles.<sup>4</sup> The most direct method involves the measurement of atom-atom scattering cross-sections as a function of incident energy and scattering angle; inversion of the data allows, in principle, a determination of the pair po-

tential at all separations. A simpler procedure is to assume a specific form for the potential and determine the parameters by fitting to the results of gas-phase measurements of quantities such as the second virial coefficient (see Chapter 3) or the shear viscosity. In this way, for example, the parameters  $\epsilon$  and  $\sigma$  in the Lennard-Jones potential have been determined for a large number of gases.

The theoretical and experimental methods we have mentioned all relate to the properties of an isolated pair of molecules. The use of the resulting pair potentials in calculations for the liquid state involves the neglect of many-body forces, an approximation that is difficult to justify. In the rare-gas liquids, the three-body, triple-dipole dispersion term is the most important many-body interaction; the net effect of triple-dipole forces is repulsive, amounting in the case of liquid argon to a few percent of the total potential energy due to pair interactions. Moreover, careful measurements, particularly those of second virial coefficients at low temperatures, have shown that the true pair potential for rare-gas atoms is not of the Lennard-Jones form, but has a deeper bowl and a weaker tail, as illustrated by the curves plotted in Figure 1.3. Apparently the success of the Lennard-Jones potential in accounting for many of the macroscopic properties of argon-like liquids is the consequence of a fortuitous cancellation of errors. A number of more accurate pair potentials have been developed for the rare gases, but their use in the calculation of condensed-phase properties requires the explicit incorporation of three-body interactions.

Although the true pair potential for rare-gas atoms is not the same as the effective pair potential used in liquid-state work, the difference is a relatively minor, quantitative one. The situation in the case of liquid metals is different, because the form of the effective ion-ion interaction is strongly influenced by the presence of a degenerate gas of conduction electrons that does not exist before the liquid is formed. The calculation of the ion-ion interaction is a complicated problem, as we shall see in Chapter 10. The ion-electron interaction is first described in terms of a “pseudopotential” that incorporates both the coulombic attraction and the repulsion due to the Pauli exclusion principle. Account

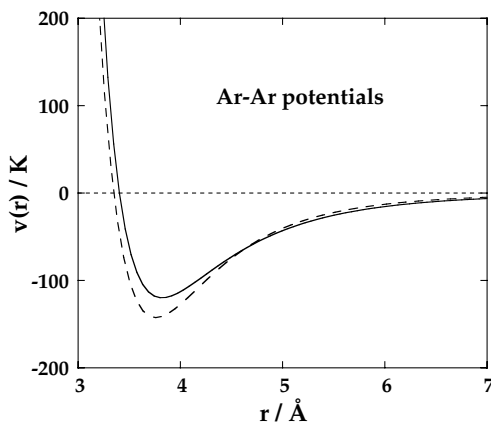


FIG. 1.3. Pair potentials for argon in temperature units. Full curve: the Lennard-Jones potential with parameter values  $\epsilon/k_B = 120$  K,  $\sigma = 3.4$  Å, which is a good effective potential for the liquid; dashes: a potential based on gas-phase data.<sup>5</sup>

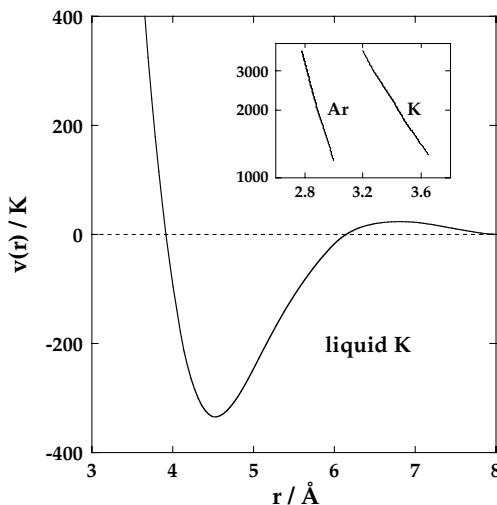


FIG. 1.4. Main figure: effective ion-ion potential (in temperature units) for liquid potassium.<sup>6</sup> Inset: comparison on a logarithmic scale of potentials for argon and potassium in the core region.

must then be taken of the way in which the pseudopotential is modified by interaction between the conduction electrons. The end result is a potential that represents the interaction between screened, electrically neutral “pseudoatoms”. Irrespective of the detailed assumptions made, the main features of the potential are always the same: a soft repulsion, a deep attractive well and a long-range oscillatory tail. The potential, and in particular the depth of the well, are strongly density dependent but only weakly dependent on temperature. Figure 1.4 shows an effective potential for liquid potassium. The differences compared with the potentials for argon are clear, both at long range and in the core region.

For molten salts and other ionic liquids in which there is no shielding of the electrostatic forces similar to that found in liquid metals, the coulombic interaction provides the dominant contribution to the interionic potential. There must, in addition, be a short-range repulsion between ions of opposite charge, without which the system would collapse, but the detailed way in which the repulsive forces are treated is of minor importance. Polarisation of the ions by the internal electric field also plays a role, but such effects are essentially many-body in nature and cannot be adequately represented by an additional term in the pair potential.

Description of the interaction between two molecules poses greater problems than for spherical particles because the pair potential is a function both of the separation of the molecules and of their mutual orientation. The model potentials discussed in this book divide into two classes. The first consists of highly idealised models of polar liquids in which a point dipole-dipole interaction is superimposed on a spherically symmetric potential. In this case the pair potential for particles labelled 1 and 2 has the general form

$$v(1, 2) = v_0(R) - \boldsymbol{\mu}_1 \cdot \boldsymbol{T}(\mathbf{R}) \cdot \boldsymbol{\mu}_2 \quad (1.2.4)$$

where  $\mathbf{R}$  is the vector separation of the molecular centres,  $v_0(R)$  is the spherically symmetric term,  $\boldsymbol{\mu}_i$  is the dipole-moment vector of particle  $i$  and  $\mathbf{T}(\mathbf{R})$  is the dipole–dipole interaction tensor:

$$\mathbf{T}(\mathbf{R}) = 3\mathbf{R}\mathbf{R}/R^5 - \mathbf{I}/R^3 \quad (1.2.5)$$

where  $\mathbf{I}$  is the unit tensor. Two examples of (1.2.4) that are of particular interest are those of dipolar hard spheres, where  $v_0(R)$  is the hard-sphere potential, and the Stockmayer potential, where  $v_0(R)$  takes the Lennard-Jones form. Both these models, together with extensions that include, for example, dipole–quadrupole and quadrupole–quadrupole terms, have received much attention from theoreticians. Their main limitation as models of real molecules is the fact that they ignore the angle dependence of the short-range forces. A simple way to take account of such effects is through the use of potentials of the second main type with which we shall be concerned. These are models in which the molecule is represented by a set of discrete *interaction sites* that are commonly, but not invariably, located at the sites of the atomic nuclei. The total potential energy of two interaction-site molecules is then obtained as the sum of spherically symmetric, interaction-site potentials. Let  $\mathbf{r}_{i\alpha}$  be the coordinates of site  $\alpha$  in molecule  $i$  and let  $\mathbf{r}_{j\beta}$  be the coordinates of site  $\beta$  in molecule  $j$ . Then the total intermolecular potential energy is

$$v(1, 2) = \frac{1}{2} \sum_{\alpha} \sum_{\beta} v_{\alpha\beta}(|\mathbf{r}_{2\beta} - \mathbf{r}_{1\alpha}|) \quad (1.2.6)$$

where  $v_{\alpha\beta}(r)$  is a site–site potential and the sums on  $\alpha$  and  $\beta$  run over all interaction sites in the respective molecules. Electrostatic interactions are easily allowed for by inclusion of coulombic terms in the site–site potentials. Let us take as an example the particularly simple case of a homonuclear diatomic, such as that pictured in Figure 1.5. A crude interaction-site model would be that of a “hard dumb-bell”, consisting of two overlapping hard spheres of diameter  $d$  with their centres separated by a distance  $L < 2d$ . This should be adequate to describe the main structural features of a liquid such as nitrogen. An obvious improvement would be to replace the hard spheres by two Lennard-Jones interaction sites, with parameters chosen to fit, say, the experimentally determined equation of state. Some homonuclear diatomics also have a large quadrupole moment, which plays a significant role in determining the short-range angular correlations in the liquid. The model could in that case be further refined by placing point charges  $q$  at the Lennard-Jones sites, together

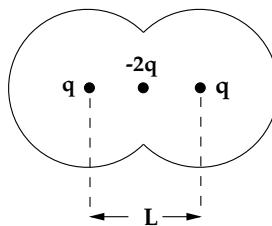


FIG. 1.5. An interaction-site model of a homonuclear diatomic.



with a compensating charge  $-2q$  at the mid-point of the internuclear bond; such a charge distribution has zero dipole moment but a non-vanishing quadrupole moment proportional to  $qL^2$ . Models of this general type have proved remarkably successful in describing the properties of a wide variety of molecular liquids, both simple and complicated.

### 1.3 EXPERIMENTAL METHODS

The experimental methods available for studying the properties of simple liquids may be placed in one of two broad categories, depending on whether they are concerned with measurements on a macroscopic or microscopic scale. In general, the calculated microscopic properties are more sensitive to the approximations used in a theory and to the assumptions made about the pair potentials, but the macroscopic properties can usually be measured with considerably greater accuracy. The two types of measurement are therefore complementary, each providing information that is useful in the development of a statistical-mechanical theory of the liquid state.

The classic macroscopic measurements are those of thermodynamic properties, particularly of the equation of state. Integration of accurate  $P$ - $\rho$ - $T$  data yields information on other thermodynamic quantities, which can be supplemented by calorimetric measurements. For most liquids the pressure is known as a function of temperature and density only in the vicinity of the liquid-vapour equilibrium line, but for certain systems of particular theoretical interest experiments have been carried out at much higher pressures; the low compressibility of a liquid near its triple point means that highly specialised techniques are required. The second main class of macroscopic measurements are those relating to transport coefficients. A variety of experimental methods are used. The shear viscosity, for example, can be determined from the observed damping of torsional oscillations or from capillary-flow experiments, while the thermal conductivity can be obtained from a steady-state measurement of the transfer of heat between a central filament and a surrounding cylinder or between parallel plates. A direct method of determining the coefficient of self-diffusion involves the use of radioactive tracers, which places it in the category of microscopic measurements; in favourable cases the diffusion coefficient can be measured by nuclear magnetic resonance (NMR). NMR and other spectroscopic methods (infrared and Raman) are also useful in the study of reorientational motion in molecular liquids, while dielectric-response measurements provide information on the slow, structural relaxation in supercooled liquids near the glass transition.

Much the most important class of microscopic measurements, at least from the theoretical point of view, are the radiation-scattering experiments. Elastic scattering of neutrons or x-rays, in which the scattering cross-section is measured as a function of momentum transfer between the radiation and the sample, is the source of our experimental knowledge of the static structure of a fluid. In the case of inelastic scattering the cross-section is measured as a function of both momentum and energy transfer. It is thereby possible to extract information on wavenumber and frequency-dependent fluctuations in liquids at wavelengths comparable with the spacing between particles. This provides a very powerful method of studying microscopic time-dependent processes in liquids. Inelastic light-scattering experiments give similar information, but the accessible range of momentum transfer limits the

method to the study of fluctuations of wavelength of order  $10^{-5}$  cm, corresponding to the hydrodynamic regime. Such experiments are, however, of considerable value in the study of colloidal dispersions and of critical phenomena.

Finally, there are a range of techniques of a quasi-experimental character, referred to collectively as computer simulation, the importance of which in the development of liquid-state theory can hardly be overstated. Simulation provides what are essentially exact results for a given potential model; its usefulness rests ultimately on the fact that a sample containing a few hundred or few thousand particles is in many cases sufficiently large to simulate the behaviour of a macroscopic system. There are two classic approaches: the *Monte Carlo* method and the method of *molecular dynamics*. There are many variants of each, but in broad terms a Monte Carlo calculation is designed to generate static configurations of the system of interest, while molecular dynamics involves the solution of the classical equations of motion of the particles. Molecular dynamics therefore has the advantage of allowing the study of time-dependent processes, but for the calculation of static properties a Monte Carlo method is often more efficient. Chapter 2 contains a brief discussion of the principles underlying the two types of calculation.

## NOTES AND REFERENCES

1. Vrij, A., Jansen, J.W., Dhont, J.K.G., Pathmamanoharan, C., Kops-Werkhoven, M.M. and Fijnaut, H.M., *Faraday Disc.* **76**, 19 (1983).
2. See, e.g., Meijer, E.J. and Frenkel, D., *Phys. Rev. Lett.* **67**, 1110 (1991). The interactions in a charge-stabilised colloidal suspension can be modelled by a Yukawa potential with a positive tail.
3. Hansen, J.P. and Verlet, L., *Phys. Rev.* **184**, 151 (1969).
4. Maitland, G.C., Rigby, M., Smith, E.B. and Wakeham, W.A., "Intermolecular Forces". Clarendon Press, Oxford, 1981.
5. Model BBMS of ref. 4, p. 497.
6. Dagens, L., Rasolt, M. and Taylor, R., *Phys. Rev. B* **11**, 2726 (1975).